Kinetics of Ligand Binding to Membrane Receptors from Equilibrium Fluctuation Analysis of Single Binding Events

Anders Gunnarsson,*,† Linda Dexlin,‡ Patric Wallin,† Sofia Svedhem,† Peter Jönsson,† Christer Wingren,‡ and Fredrik Höök*,†

†Department of Applied Physics, Chalmers University of Technology, SE-41133 Göteborg, Sweden
‡Department of Immunotechnology and CREATE Health, Lund University, SE-221 84 Lund, Sweden

S *Supporting Information*

ABSTRACT: Equilibrium fluctuation analysis of single binding events has been used to extract binding kinetics of ligand interactions with cell-membrane bound receptors. Time-dependent total internal reflection fluorescence (TIRF) imaging was used to extract residence-time statistics of fluorescently stained liposomes derived directly from cell membranes upon their binding to surface-immobilized antibody fragments. The dissociation rate constants for two pharmaceutical relevant antibodies directed against different B-cell expressed membrane proteins was clearly discriminated, and the affinity of the interaction could be determined by inhibiting the interaction with increasing concentrations of soluble antibodies. The single-molecule sensitivity made the analysis possible without overexpressed membrane proteins, which makes the assay attractive in early drug-screening applications.

Two-thirds of the existing drugs are directed against plasma-membrane proteins.[1] The identification of new low-molecular weight drugs[2] and pharmaceutical antibodies[3] that interact with this class of proteins has therefore become a vital part of the drug discovery process. Such drug-target identification is often quantified *in vitro* by interaction parameters such as the half maximal inhibitory concentration, IC_{50}, or the equilibrium dissociation constant, K_d. However, since *in vivo* drug binding occurs under transient, nonequilibrium, conditions, the importance of binding kinetics, and in particular the residence time ($\tau = 1/k_{off}$) of the drug-target interaction, is being increasingly recognized as a key parameter in evaluating both drug efficacy and toxicity.[4−8] Hence, screening assays that rely on IC_{50} or K_d determinations do not necessarily provide the most relevant information to assess the potency of drug candidates.[9]

Recently, surface-sensitive techniques, such as surface plasmon resonance (SPR) spectroscopy, combined with controlled liquid-flow conditions, have been successively applied to probe binding kinetics of drug candidates to surface-immobilized water-soluble drug targets.[10−12] Significant efforts have therefore been undertaken to transfer this approach into analogous screening assays for cell-membrane-associated receptors. However, the low concentrations of membrane receptors in cell membranes and the need to preserve their natural hydrophobic environment in reconstituted surface-supported lipid membranes often result in low receptor densities accompanied with low signal-to-noise (S/N) levels. To increase the surface concentration of immobilized membrane receptors various strategies, including membrane protein presenting virus particles,[13] reconstituted membrane proteins in amphipathic polymers,[14] and planar lipid bilayers,[15] have been developed. Encouraging results have indeed been reported, including antibody binding to cytochrome b_6f and bc_1[14] and chemokine receptors.[13] However, to this end these approaches are practically cumbersome, still provide low S/N levels, and/or suffer from not preserving the natural cell membrane environment.[16] The *in vitro* assays generally used to screen ligands directed against membrane receptors therefore employ dye-labeled ligands in competition assays that rely on fluorescence readout. Typically, binding assays using plasma membrane fragments[17] or whole cell imaging[18] are performed under stagnant liquid conditions in microtiter plate formats. However, these assays do not enable extraction of kinetic data, but rather IC_{50} or K_d.

We present in this work a microtiter plate assay that operates under stagnant liquid conditions without sacrificing the possibility to provide kinetic information of cell membrane receptor—ligand interactions. The principle is schematically illustrated in Figure 1, which shows how single binding events of fluorescently stained membrane-receptor containing liposomes to a ligand-modified microwell surface can be monitored using time-resolved TIRF imaging. Facilitated by the evanescent field illumination, the residence time of binding, and thus the dissociation kinetics of bound liposomes, can be obtained under equilibrium binding conditions in a *stagnant* liquid, despite the presence of suspended liposomes in the solution.[19]

A related method that is also capable of extracting ligand binding kinetics to cell membrane receptors under stagnant conditions is fluorescence correlation spectroscopy (FCS).[20] Although more widely applied for whole cell[21] rather than proteoliposome[22] analysis, kinetic rate constants can be obtained from the ability to temporally resolve the relative amounts of free and bound fluorescently labeled ligands. FCS has also been combined with TIR illumination to study interactions at surfaces.[23] However, ligand concentrations in the nM range are typically needed to obtain k_{on} and K_d constants, while competitive binding using a large excess (typically > μM) of unlabeled ligands is required to extract k_{off}.[24]

We here demonstrate that it is possible to obtain kinetic information of cell membrane receptor—ligand interactions using a surface-based format by immobilizing a small amount
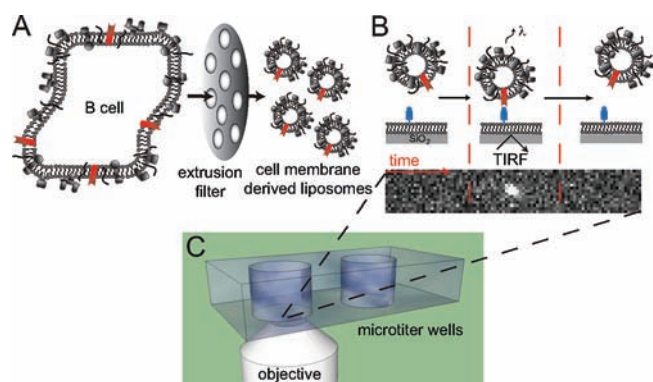
Figure 1. (A) Schematic illustration of the preparation of cell membrane derived liposomes by extrusion through a filter. (B) The fluorescently stained liposomes carrying the membrane receptor of interest (red) associate and dissociate from the surface immobilized ligand (blue) at equilibrium binding conditions. (C) Each individual association and dissociation event is monitored over time by TIRF microscopy in a microwell format.
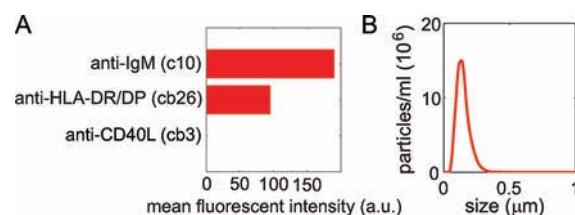

Figure 2. (A) FACS analysis of intact cells prior to liposome generation, confirming the plasma membrane expression of the targeted receptors, IgM and HLA-DR/DP. An additional scFv antibody directed against CD40L (clone cb3), a membrane receptor not expressed by the B-cells, shows no binding. (B) Typical size distribution of extruded cell membrane derived liposomes obtained by nanoparticle tracking analysis.

(fmol) of the ligand on a surface. Combined with evanescent-wave excitation of receptor-containing fluorescently stained liposomes, the method is used to quantify the dissociation kinetics of membrane receptor–ligand interactions at low pM liposome concentrations. We also demonstrate how the assay, which can easily be further miniaturized and adopted to multiplexed analysis, can be used to determine equilibrium binding constants, K_d, as well as a rough estimate of the average amount of receptors per liposome. In analogy with solution assays employed in drug-screening applications, the latter numbers were obtained by inhibiting the liposome binding to the ligand-modified substrate using suspended ligands at sub-μM concentrations.

Two high-performing human recombinant single chain Fv (scFv) antibodies (clone c10 and cb26),[25] selected from the n-CoDeR library,[26] were directed against two key immunological plasma membrane receptors: IgM (which is an antigen receptor on B-cells; vital for activation of the B-cell) and HLA-DR/DP (which displays processed antigens in the format of peptides on antigen presenting cells, vital for activation of T-cells) were coupled to a planar supported lipid bilayer (see Supporting Information, SI). Besides providing an inert background that prevents non-specific liposome binding,[27] a small fraction of chemically active lipids offer a gentle means to immobilize ligands without significantly altering their function.

Liposomes derived from the cell membrane of B-cells were produced by extruding the cell suspension through polycarbonate membranes directly after plasma membrane staining of the intact cells with a fluorescent lipophilic dye (see SI). Prior to cell disruption and labeling, the presence of the two membrane receptors on the cell surface was confirmed by fluorescent automated cell sorting (FACS) analysis (Figure 2A) using fluorescently labeled secondary (anti-His-tag) antibodies. The concentration and size distribution of a typical batch of extruded cell membrane derived liposomes was determined, using nanoparticle tracking analysis to 30 pM and 150 ± 50 nm (Figure 2B), respectively. A fraction of the liposomes may be derived from subcellular components, which implies that the concentration of liposomes available for binding is somewhat lower.

Standard protocols for production of cell membrane derived liposomes, such as plasma membrane vesiculation[28] or sonication,[29]

typically include multiple purification and enrichment steps.[30] In contrast to these protocols, a nonpurified or enriched suspension of liposomes derived directly from extruded cells may contain compounds that interfere with the surface interaction. The simplified preparation protocol adds a significant practical advantage, but the complexity of the liposome suspension puts additional demands on the surface chemistry to avoid unspecific binding reactions. Out of multiple surface chemistries, including carboxyl end-capped thiol-poly(ethylene glycol) [SH-PEG$_X$-COOH] with 0.5 kDa or 5 kDa PEG spacers, a scFv-modified supported lipid bilayer was shown to generate sufficiently low nonspecific binding reactions of the crude liposome suspension for kinetics of cell membrane derived liposome binding to be unambiguously extracted. The surface modification protocol was verified in situ using the quartz crystal microbalance with dissipation (QCM-D) monitoring technique, which also served to demonstrate successful antibody immobilization and specific detection of membrane receptor containing liposomes (see Figure S1 in SI).

A typical residence time histogram displaying the number of liposomes that remained bound for a certain time interval, $t + \Delta t$ ($\Delta t = 20$ s), is shown in Figure 3B. When extracting the dissociation time constant, this graph was for simplicity converted into a dissociation curve displaying the number of liposomes that remained bound to the substrate after a given time (Figure 3C). This plot thus represents the same type of graph typically obtained by monitoring the dissociation process upon rinsing in conventional surface-based biosensor formats, but here instead obtained in a stagnant liquid. The negative control surface (without ligand) shows few binding and release events, verifying successful surface modification (Figure 3C). From single exponential fits, the dissociation rate constants, k_{off}, were determined to $(1.6 \pm 0.2) \times 10^{-3}$ s^{-1} ($n = 3$) and $(2.6 \pm 0.6) \times 10^{-3}$ s^{-1} ($n = 3$) for the interaction between the IgM receptor and the scFv antibody (clone c10) and the HLA-DR/DP receptor and scFv antibody (clone cb26), respectively (Figure 3C). Note the kinetic analysis was based on in total no more than about 100 liposomes. The k_{off} values remained constant for different liposome sizes and at different ligand densities (Figure S2). These values are also in good agreement with the dissociation rate constants previously reported for scFv interactions when directed against water-soluble compounds,[31] but were not yet reported for similar clones directed against cell-membrane receptors.

In the analysis, only liposomes that dissociate at some point during the measurement are taken into account. This thus constitutes an efficient means to filter out irreversibly bound
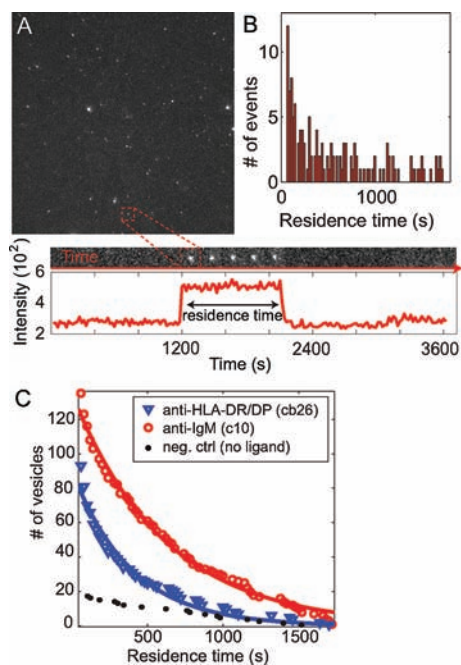
14853

dx.doi.org/10.1021/ja2047039 |*J. Am. Chem. Soc.* 2011, 133, 14852–14855

Figure 3. (A) Fluorescence micrograph snapshot and kymograph (displaying every 10th frame) with corresponding intensity profile of a small subsection $(6 \times 6 \, \mu m^2)$, highlighting a single liposome interacting with the surface immobilized ligand. Detection of individual binding events was obtained by distinguishing bound liposomes from noninteracting liposomes that disappear from the surface during the time between two consecutive frames (see SI for details on the image analysis). (B) Residence time histogram generated from a measurement of around 100 lipid vesicles. (C) Typical dissociation trends for the two different membrane receptor–ligand interactions and the negative control (no ligand), plotted as the number of liposomes that still remain bound after a certain time. The dissociation rates were fitted (solid lines) to single exponential functions.

liposomes (see also Figure S1). In fact, around 80% of the detected liposomes remained irreversibly bound over these time scales. A likely explanation to this observation is that a significant fraction of the liposomes contain more than one receptor, thus resulting in multivalent interactions that are irreversible on the time scale of the measurement. This interpretation is further supported by the good agreement between the observed k_{off} values and previously reported dissociation rate constants for similar scFv interactions.[31] Since multivalent interactions have been shown to increase the residence time by a factor of 20 or more,[32,33] this suggests that the population of liposomes that exhibit reversible binding interact with a single recognition element (see further below). This is further supported by a relative increase in the number of release events over irreversibly bound liposomes upon a 10-fold decrease in ligand density (Figure S2 in SI).

Under the assumption that the association rate constants, k_{on}, are similar for different scFv antibodies from the same library,[31] the measured k_{off} values suggest K_d values for the two clones of around 5 nM (clone cb26) and 3 nM (clone c10). To independently estimate K_d we monitored the decrease in the rate of bound liposomes, dN_+/dt, in the presence of increasing concentrations of suspended scFv (Figure 4A).

Liposomes preincubated with suspended ligand rapidly reach linear binding rates with lower slopes at increasing ligand
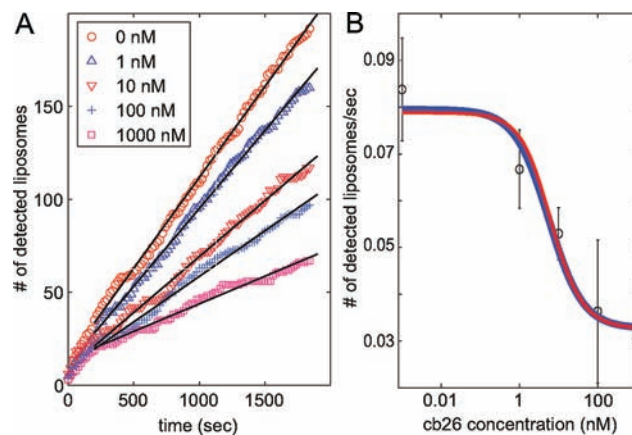

Figure 4. (A) Inhibition assay: number of detected liposomes as a function of time in the presence of increasing concentrations of suspended ligand (cb26) including linear fits from the point in time when equilibrium was established. (B) Slope of the linear fits in (A) versus concentration of suspended ligand. The fits in (B) correspond to the modified expression (eq 1) assuming a Poisson distribution of receptors per liposomes with the average number of 0.23 (blue) and 2.5 (red) receptors.

concentration. At the liposome concentrations (pM) used in these experiments, the surface coverage is well below saturation. This means that, at equilibrium binding conditions, the rate of binding is expected to be constant, with slopes that directly reflect the concentration of liposomes that carries at least one receptor. In the ideal case, in which the liposomes contain a single receptor each, the decrease in rate of binding as a function of ligand concentration can be represented with a Langmuir isotherm.[34] However, the number of receptors per liposome is in this case expected to follow a Poisson distribution. Under this assumption, the rate of bound liposomes can be expressed as (see SI for derivation):

$$\frac{dN_+}{dt} = A \left(1 - \exp\left(-\frac{\langle n \rangle}{1 + C_{ligand}/K_d} \right) \right) \quad (1)$$

where A is a constant, $\langle n \rangle$ is the average number of receptors per liposomes, and C_{ligand} is the concentration of suspended ligand. Using a K_d of 5 nM as estimated above for clone cb26, the best fit is obtained for $\langle n \rangle = 0.23$ (blue fit in Figure 4B). However, at this value of $\langle n \rangle$, the fraction of liposomes with more than one receptor is only a few percent, which is significantly lower than the observed irreversible fraction of 80% previously attributed to multivalent binding. By instead matching the receptor distribution to the observation that 20% of the liposomes are reversibly bound (one receptor per liposome) and approximately 80% have more than one receptor, $\langle n \rangle$ becomes 2.5, with a best fit obtained for a K_d of 2 nM (red fit in Figure 4B).

Although the uncertainty in the receptor distribution translates into an uncertainty in the determination of K_d, a 2 to 5 nM interval is in good agreement with the expectation for this class of antibodies.[31] Also note that k_{off} remained the same for the fraction of bound liposomes during the inhibition experiment. Together with the reasonably good agreement between the estimated K_d from the inhibition analysis and that obtained from k_{off} and literature data on k_{on}, this further supports that the reversible fraction of liposomes corresponds to single receptor interactions. Most importantly, the determination of k_{off}, which is

considered the most important parameter in order to determine the potency of drug candidates,[4] can be very accurately determined already at low pM concentrations of liposomes.[35]

In conclusion, the high sensitivity of the assay eliminates the need for membrane-receptor overexpression and/or purification procedures, which are typically employed in conventional membrane-protein assays. This is particularly important from the perspective of translating the assay to other types of ligand—receptor interactions, in which case concerns are often raised regarding the influence on protein function upon overexpression,[36] reconstitution into liposomes,[37] and surface immobilization.[38] Furthermore, the assay allows parallel dispensing of suspended cell-membrane-derived liposomes in multiple microtiter wells or on surface-based arrays, followed by either serial or parallel readout. Hence, the assay could be directly transferable to high-throughput screening applications, which is especially attractive owing to the low concentration ($\leq$pM) and small total sample consumption ($\leq$fmol) needed for the dissociation kinetic analysis. Finally, the self-incorporated label used to visualize the liposomes is a standard fluorescent dye used primarily for staining of living cells. The labeling is thus likely to have minimal influence on the structure and function of the actual membrane receptors. Still, the number of dyes per liposome was sufficiently high not to impose photobleaching (see intensity profile in Figure 3A), which otherwise tends to limit single-molecule *imaging* techniques, in which the molecule of interest is directly labeled, to low affinity interactions ($k_{off} > 10^{-1} \text{ s}^{-1}$).[39]

■ ASSOCIATED CONTENT

Ⓢ Supporting Information. Supporting Information contains the derivation of the expression in eq 1, complementary QCM-D data for the antibody-immobilization protocol, additional experimental details and complete ref 34. This material is available free of charge via the Internet at http://pubs.acs.org.

■ AUTHOR INFORMATION

Corresponding Author
anders.gunnarsson@chalmers.se; fredrik.hook@chalmers.se

■ ACKNOWLEDGMENT

■ REFERENCES

(1) Josic, D.; Clifton, J. G. *Proteomics* **2007**, *7*, 3010–3029.
(2) Schreiber, S. L. *Science* **2000**, *287*, 1964–1969.
(3) Nieri, P.; Donadio, E.; Rossi, S.; Adinolfi, B.; Podesta, A. *Curr. Med. Chem.* **2009**, *16*, 753–779.
(4) Copeland, R. A.; Pompliano, D. L.; Meek, T. D. *Nat. Rev. Drug Discovery* **2006**, *5*, 730–739.
(5) Zhang, R.; Monsma, F. *Curr. Opin. Drug Discovery Dev.* **2009**, *12*, 488–496.
(6) Gabrielsson, J.; Dolgos, H.; Gillberg, P. G.; Bredberg, U.; Benthem, B.; Duker, G. *Drug Discov. Today* **2009**, *14*, 358–372.
(7) Lu, H.; Tonge, P. J. *Curr. Opin. Chem. Biol.* **2010**, *14*, 467–474.
(8) Swinney, D. C. *Curr. Opin. Drug Discovery Dev.* **2009**, *12*, 31–39.
(9) Kenakin, T. *ACS Chem. Biol.* **2009**, *4*, 249–260.
(10) Karlsson, R.; Michaelsson, A.; Mattsson, L. *J. Immunol. Methods* **1991**, *145*, 229–240.

(11) Karlsson, R.; Kullman-Magnusson, M.; Hamalainen, M. D.; Remaeus, A.; Andersson, K.; Borg, P.; Gyzander, E.; Deinum, J. *Anal. Biochem.* **2000**, *278*, 1–13.
(12) Huber, W.; Mueller, F. *Curr. Pharm. Des.* **2006**, *12*, 3999–4021.
(13) Hoffman, T. L.; Canziani, G.; Jia, L.; Rucker, J.; Doms, R. W. *Proc. Natl. Acad. Sci. U.S.A.* **2000**, *97*, 11215–11220.
(14) Charvolin, D.; Perez, J. B.; Rouviera, F.; Giusti, F.; Bazzacco, P.; Abdine, A.; Rappaport, F.; Martinez, K. L.; Popot, J. L. *Proc. Natl. Acad. Sci. U.S.A.* **2009**, *106*, 405–410.
(15) Karlsson, O. P.; Lofas, S. *Anal. Biochem.* **2002**, *300*, 132–138.
(16) Lingwood, D.; Simons, K. *Science* **2010**, *327*, 46–50.
(17) *Protein-Ligand Interactions; Methods and Applications*; Nienhaus, G. U., Ed.; Humana Press: 2005; Vol. 305.
(18) Lang, P.; Yeow, K.; Nichols, A.; Scheer, A. *Nat. Rev. Drug Discovery* **2006**, *5*, 343–356.
(19) Gunnarsson, A.; Jonsson, P.; Zhdanov, V. P.; Hook, F. *Nucleic Acids Res.* **2009**, *37*, e99.
(20) Briddon, S. J.; Hill, S. J. *Trends Pharmacol. Sci.* **2007**, *28*, 637–645.
(21) Pramanik, A. *Curr. Pharm. Biotechnol.* **2004**, *5*, 205–212.
(22) Schuler, J.; Frank, J.; Trier, U.; Schafer-Korting, M.; Saenger, W. A. *Biochemistry* **1999**, *38*, 8402–8408.
(23) Lieto, A. M.; Cush, R. C.; Starr, T. E.; Thompson, N. L. *Biophys. J.* **2003**, *84*, 587a–587a.
(24) Pramanik, A.; Olsson, M.; Langel, U.; Bartfai, T.; Rigler, R. *Biochemistry* **2001**, *40*, 10839–10845.
(25) Dexlin, L.; Ingvarsson, J.; Frendeus, B.; Borrebaeck, C. A. K.; Wingren, C. *J Proteome Res.* **2008**, *7*, 319–327.
(26) Soderlind, E.; Strandberg, L.; Jirholt, P.; Kobayashi, N.; Alexeiva, V.; Aberg, A. M.; Nilsson, A.; Jansson, B.; Ohlin, M.; Wingren, C.; Danielsson, L.; Carlsson, R.; Borrebaeck, C. A. K. *Nat. Biotechnol.* **2000**, *18*, 852–856.
(27) Glasmastar, K.; Larsson, C.; Hook, F.; Kasemo, B. *J. Colloid Interface Sci.* **2002**, *246*, 40–47.
(28) Scott, R. E. *Science* **1976**, *194*, 743–745.
(29) Larsson, C.; Widell, S.; Kjellbom, P. *Method Enzymol* **1987**, *148*, 558–568.
(30) Cordwell, S. J.; Thingholm, T. E. *Proteomics* **2010**, *10*, 611–627.
(31) Ellmark, P.; Esteban, O.; Furebring, C.; Hager, A. C. M.; Ohlin, M. *Mol. Immunol.* **2002**, *39*, 349–356.
(32) Howorka, S.; Nam, J.; Bayley, H.; Kahne, D. *Angew. Chem., Int. Ed.* **2004**, *43*, 842–846.
(33) Plant, A. L.; Gray, M.; Hubbard, J. B. *Biophys. Chem.* **1993**, *48*, 75–89.
(34) Thorsen, T. S.; et al. *Proc. Natl. Acad. Sci. U.S.A.* **2010**, *107*, 413–418.
(35) Gunnarsson, A.; Jonsson, P.; Marie, R.; Tegenfeldt, J. O.; Hook, F. *Nano Lett.* **2008**, *8*, 183–188.
(36) Wagner, S.; Baars, L.; Ytterberg, A. J.; Klussmeier, A.; Wagner, C. S.; Nord, O.; Nygren, P. A.; van Wijk, K. J.; de Gier, J. W. *Mol. Cell Proteomics* **2007**, *6*, 1527–1550.
(37) Phillips, R.; Ursell, T.; Wiggins, P.; Sens, P. *Nature* **2009**, *459*, 379–385.
(38) Chan, Y. H. M.; Boxer, S. G. *Curr. Opin. Chem. Biol.* **2007**, *11*, 581–587.
(39) Morimatsu, M.; Takagi, H.; Ota, K. G.; Iwamoto, R.; Yanagida, T.; Sako, Y. *Proc. Natl. Acad. Sci. U.S.A.* **2007**, *104*, 18013–18018.